ARTICLE

Journal of Cellular Biochemistry 113:2442–2450 (2012)

Journal of Cellular Biochemistry

The Plating of Rat Scar Myofibroblasts on Matrigel Unmasks a Novel Phenotype; the Self Assembly of Lumen-Like Structures

Viviane El-Helou,[1] Hugues Gosselin,[2] Louis Villeneuve,[2] and Angelino Calderone[1,2]*

[1]*Département de Physiologie, Université de Montréal, Montréal, Québec, Canada*

[2]*Montreal Heart Institute, Montreal, Quebec, Canada*

ABSTRACT

During tissue healing, the primary role of myofibroblasts involves the synthesis and deposition of collagen. However, it has also been reported that selective populations of myofibroblasts can acquire the phenotype and/or differentiate to other cells types. The present study tested the hypothesis that myofibroblasts isolated from the scar of the ischemically damaged rat heart can recapitulate an endothelial cell-like response when plated in a permissive in vitro environment. Scar myofibroblasts, neonatal and adult ventricular fibroblasts express smooth muscle α-actin, collagen α_1 type 1 and a panel of pro-fibrotic and pro-angiogenic peptide growth factor mRNAs. Myofibroblasts plated alone on matrigel led to the self assembly of lumen-like structures whereas neonatal and adult rat ventricular fibroblasts were unresponsive. Myofibroblasts labeled with the fluorescent cell tracker CM-DiI were injected in the viable myocardium of 3-day post-myocardial infarcted Sprague–Dawley rats and sacrificed 7 days later. Injected CM-DiI-labeled myofibroblasts were detected predominantly in the peri-infarct/infarct region, highlighting their migration to the damaged region. However, engrafted myofibroblasts in the peri-infarct/infarct region were unable to adopt an endothelial cell-like phenotype or lead to the de novo formation of CM-DiI-labeled blood vessels. The non-permissive nature of the infarct region may be attributed at least in part to the presence of growth-promoting stimuli as TGF-β and the β-adrenergic agonist isoproterenol inhibited the self assembly of lumen-like structures by myofibroblasts. Thus, when plated in a permissive in vitro environment, scar myofibroblasts can self assemble and form lumen-like structures providing an additional novel phenotype distinguishing this population from normal ventricular fibroblasts. J. Cell. Biochem. 113: 2442–2450, 2012. © 2012 Wiley Periodicals, Inc.

KEY WORDS: CORONARY ARTERY DISEASE; REMODELLING; ANGIOGENESIS; FIBROBLASTS; INFARCT

Following an ischemic insult to the heart, the healing process is denoted as reparative fibrosis and represents an essential physiological response to repair the damaged myocardium [Sun et al., 2000; Frangogiannis et al., 2002; Virag and Murry, 2003]. Although, the reparative fibrotic response requires the interaction of several biological events, myofibroblasts play a seminal role. Myofibroblasts express smooth muscle α-actin$^{(+)}$ and the intermediate filament protein nestin, and compared to normal adult ventricular fibroblasts, have a higher proliferative rate and synthesize greater amounts of collagen [Willems et al., 1994; Squires et al., 2005; Wynn, 2008; Beguin et al., 2012]. Physiologically, the scar limits cardiac myocyte slippage and left ventricular dilatation. Consequently, inadequate scar healing related in part to decreased collagen deposition and/or reduced myofibroblast proliferation leads to infarct thinning, chamber expansion and adverse cardiac remodelling [Dai et al., 2005; Cimini et al., 2007; van Amerongen et al., 2008; El-Helou et al., 2008b; Liam et al., 2009; Pilla et al., 2009]. Myofibroblasts may further participate in reparative neovascularization and sympathetic fibre innervation of the peri-infarct/infarct region via the synthesis and release of angiogenic and neurotrophic stimuli [Micera et al., 2001; Zhao and Eghbali-Webb, 2001; Chintalgattu et al., 2003; Hasan et al., 2006; El-Helou et al., 2008b]. Several studies have reported that select populations of fibroblasts/myofibroblasts can inherently or following genetic reprogramming acquire the phenotype and/or differentiate to other cell types. Spindle-shaped, smooth muscle α-actin$^{(+)}$ myofibroblasts isolated from the human placenta and cultured in a permissive environment differentiated to adipocytes, osteoblasts, and chrondocytes [Strakova et al., 2008]. The overexpression of the ephrin A5 receptor in NIH3T3 fibroblasts induced an endothelial cell-like response when plated on

Grant sponsor: Heart and Stroke Foundation of Canada and Quebec; Grant sponsor: Canadian Diabetes Association.

*Correspondence to: Angelino Calderone, Research Centre, Institut de Cardiologie de Montréal, 5000 rue Bélanger Est, Montréal, QC, Canada H1T 1C8. E-mail: angelo.calderone@umontreal.ca

Manuscript Received: 17 January 2012; Manuscript Accepted: 24 February 2012

Accepted manuscript online in Wiley Online Library (wileyonlinelibrary.com): 2 March 2012

DOI 10.1002/jcb.24117 • © 2012 Wiley Periodicals, Inc.

matrigel [Campbell et al., 2006]. The selective loss of caveolin-1 in human mammary stromal fibroblasts led to a cancer-associated fibroblast phenotype and the recapitulation of an endothelial cell-like response in vitro characterized by the self assembly of lumen-like structures on matrigel [Sotgia et al., 2009]. Therefore, the present study tested the hypothesis that myofibroblasts isolated from the infarct region of the ischemically damaged rat heart can recapitulate an endothelial cell-like response by forming lumen-like structures when plated on matrigel.

METHODS

MYOCARDIAL INFARCT MODEL AND ISOLATION OF SCAR MYOFIBROBLASTS AND VENTRICULAR FIBROBLASTS

Myocardial infarction (MI) was induced in male Sprague–Dawley rats (9–11 weeks old; Charles Rivers, St. Constant, Canada) following ligation of the left anterior descending coronary artery as previously described [Geraldes et al., 2007]. Scar myofibroblasts were isolated from the infarct region of 1-week post-MI male rats and adult cardiac fibroblasts isolated from the left ventricle of normal male Sprague–Dawley rats (9–11 weeks old; Charles Rivers), as previously described [Calderone et al., 2006; Beguin et al., 2012]. Neonatal fibroblasts were isolated from 1- to 3-day-old Sprague–Dawley pups (Charles Rivers), as previously described [Colombo et al., 2003; Beguin et al., 2012]. Regardless their source, fibroblasts were cultured in an identical fashion and experiments performed on 1st passage cells, unless otherwise indicated. For Western blot and real-time PCR experiments, first passage scar myofibroblasts, adult, and neonatal fibroblasts were plated at a density of 125–150 cells/mm^2 and kept in DMEM supplemented with 7% FBS for 2 and 7 days, respectively. Cells were subsequently washed; the media replaced with serum-free DMEM containing insulin (5 μg/ml), transferrin (5 μg/ml), and selenium (5 ng/ml), and harvested 2 days later following experimental protocol. The use and care of laboratory animals was according to the Canadian Council for Animal Care and each experimental protocol was approved by the Animal Care Ethics Committee of the Montreal Heart Institute.

WESTERN BLOT ANALYSIS

Protein lysate (50–100 μg) obtained from cultured fibroblast/myofibroblasts and the normal rat aorta ($n = 3$) was subjected to SDS–polyacrylamide gel (10%) electrophoresis, and subsequently transferred to a PVDF membrane (Perkin Elmer Life Sciences, Boston, MA) [Beguin et al., 2012]. Antibodies used include a mouse monoclonal anti-smooth muscle α-actin (1:2,000; Sigma–Aldrich, St. Louis, MI); mouse monoclonal anti-GAPDH (1:10,000; Ambion), a goat polyclonal anti-VE-cadherin (1:500; Santa Cruz Biotechnology, CA); a mouse monoclonal anti-endothelial nitric oxide synthase (eNOS; 1:500; BD Biosciences, Mississauga, ON) and appropriate secondary IgG antibodies conjugated to horseradish peroxidase (1:10,000 Santa Cruz Biotechnology). The immunoreactive signal was visualized by an ECL detection kit (Perkin Elmer). Films were scanned with Image J software® and the target protein signal was depicted as arbitrary light units normalized to GAPDH protein.

REAL-TIME PCR

RT-PCR and real-time PCR were performed as previously described [El-Helou et al., 2008B]. The primers used were rat vascular endothelial growth factor-A (VEGF-A), forward 5′-GAAATCCC-GGTTTAAATCCTGG-3′ and reverse 5′-CGCTCTGAACAAGGCTCA-CAG-3′; rat transforming growth factor-β_1 (TGF-β_1), forward 5′-TGCTAATGGTGGACCGCAA-3′ and reverse 5′-TGATGTCTTT-GGTTTTGTCATAGATTG-3′; rat transforming growth factor-β_3 (TGF-β_3), forward 5′-AGAGATCCATAAATTCGACAT-3′ and reverse 5′-ACACATTGAAACGGAAAACCT-3′; rat connective tissue growth factor (CTGF), forward 5′-AGGCCCTGTGAAGCTGACCTAGA-3′ and reverse 5′-TTTTAGGCGTCCGGATGCACT-3′; rat collagen ?1 type 1 forward, 5′-ggacctggtttcttctcaccc-3′ and reverse 5′-AGGTAGTTG-CATCCCAATTCA-3′ and rat β-actin forward 5′-CCCTAAGGC-CAACCGTGAA-3′ and reverse 5′-GAGGCATACAGGGACAACAC-AG-3′. mRNA levels were normalized to β-actin mRNA.

DNA AND PROTEIN SYNTHESIS

First passage scar myofibroblasts (125 cells/mm^2) were treated with isoproterenol (1 μM; Sigma–Aldrich) or TGF-β_3 (0.001–1 ng/ml; R&D Systems; Minneapolis, MN) for 24 h. In separate experiments, the phosphatidylinositol 3-kinase (PI3-K) inhibitor LY294002 (10 μM; Biomol International, Plymouth Meeting, PA), or the mammalian target of rapamycin (mTOR) inhibitor rapamycin (10 nM; Biomol International) was added alone or 15–30 min prior to the addition of isoproterenol and DNA and protein synthesis were assessed 24 h later, as previously described [Colombo et al., 2003; Calderone et al., 2006; Beguin et al., 2012].

MATRIGEL ASSAY

Ice-cold matrigel (100 μl; BD Biosciences) poured in 24-well plates was allowed to solidify for 30 min at 37°C, as previously described [Geraldes et al., 2007]. First, 2nd, or 3rd passage myofibrolasts, 1st passage neonatal and adult ventricular fibroblasts (25,000 cells/well of a 24-well plate) were plated on matrigel in the absence or presence of TGF-β_1 (1 ng/ml), TGF-β_3 (1 ng/ml), or TGF-β R1 kinase inhibitor II (100 nM; a cell-permeable and selective ATP-competitive inhibitor of TGF-β type I receptor; Calbiochem, La Jolla, CA). Lumen-like structure formation was examined 2–4, 8, and 24 h after the initial plating. For each experiment, phase contrast pictures were taken of five fields and the number of lumen-like structures counted.

IN VIVO INJECTION OF SCAR MYOFIBROBLASTS IN POST-MI RATS AND IMMUNOFLUORESCENCE

First passage scar myofibroblasts were trypsinized and 1×10^6 cells injected with a Hamilton syringe (30 G; 10 μl volume) at four distinct sites in the viable myocardium in close proximity to the peri-infarct/infarct region of 3-day post-MI rats ($n = 4$). To track their migration and differentiation in vivo, injected cells were labeled with the fluorescent cell tracker CM-DiI. (excitation/emission 553/570 nm; Invitrogen, Eugene, OR). Seven days after injection, MI rats were sacrificed, the heart excised, immersed in 2-methyl butane and stored at −80°C. In rat hearts grafted with CM-DiI-labeled myofibroblasts, staining was performed on tissue cryocuts of 14 μM thickness, as previously described [El-Helou

et al., 2008a]. The antibodies employed were a mouse monoclonal anti-eNOS (1:100, BD Biosciences), mouse monoclonal anti-smooth muscle α-actin (1:100; Sigma–Aldrich) and a goat anti-mouse IgG conjugated to Alexa-488 (1:600; InVitrogen; emission wavelength, 520 nm). The nucleus was identified with To-PRO3 staining (InVitrogen; 1.5 μM; emission wavelength, 661 nm) [Hasan et al., 2006; Strakova et al., 2008]. An immunoreactive signal was not detected in tissue incubated with conjugated secondary antibody alone. F-actin filament staining was detected with phalloidin-conjugated Alexa-555 (1:200; InVitrogen) in scar myofibroblasts plated at a density of 125 cells/mm^2 in serum DMEM supplemented with 7% FBS for 2 days. Cells were subsequently washed; the media replaced with serum-free DMEM containing insulin (5 μg/ml), transferrin (5 μg/ml), and selenium (5 ng/ml), and treated 2 days later with isoproterenol (1 μM) or TGF-β_1 (1 ng/ml). Immunofluorescence staining was visualized with a 10×- or 63×-oil 1.4 NA DIC plan apochromat objective mounted on a Zeiss Axiovert 100 M confocal microscope.

STATISTICS

Data are expressed as the mean ± SEM and each "n" represents the number of rats or individual fibroblast preparations. A Students' unpaired *t*-test or one-way analysis of variance (ANOVA) was performed (GraphPad Prism, San Diego, CA). For a one-way ANOVA, a significant difference was determined by the Student–Newman–Keuls Multiple Comparisons post hoc test and a *P*-value < 0.05 was considered statistically significant for each test.

RESULTS

THE PHENOTYPE OF SCAR MYOFIBROBLASTS AND NORMAL VENTRICULAR FIBROBLASTS

Smooth muscle α-actin protein (1.45 ± 0.3; n = 3 and normalized to GAPDH protein) and collagen α_1 type 1 mRNA were expressed in cultured myofibroblasts isolated from the infarct region of 1-week post-MI rats (Fig. 1 and Table I). Scar myofibroblasts also express a panel of pro-fibrotic and pro-angiogenic peptide growth factor mRNAs (normalized to β-actin mRNA) including, TGF-β_1, TGF-β_3, CTGF, and VEGF-A (Table I). Smooth muscle α-actin protein was expressed by neonatal (1.1 ± 0.02; n = 3) and adult ventricular fibroblasts (1.0 ± 0.15; n = 3) isolated from normal rat hearts and level of expression was similar to scar myofibroblasts (Fig. 1). Collagen α_1 type 1 mRNA levels in adult fibroblasts were

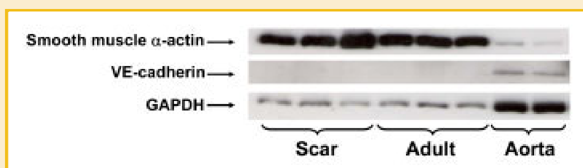

Fig. 1. Smooth muscle α-actin and VE-cadherin expression in cardiac fibroblasts. Smooth muscle α-actin protein expression was comparable in scar myofibroblasts (Scar; n = 3) and adult ventricular fibroblasts (Adult; n = 3). By contrast, VE-cadherin protein expression in the aorta (n = 3) was not detected in myofibroblasts and adult ventricular fibroblasts. Protein expression was normalized to GAPDH protein.

significantly lower than neonatal fibroblasts and scar myofibroblasts (Table I). VEGF-A and TGF-β_3 mRNA levels were comparable in neonatal and adult ventricular fibroblasts but significantly lower than myofibroblasts (Table I). By contrast, CTGF and TGF-β_1 mRNA levels were similar in myofibroblasts, neonatal and adult ventricular fibroblasts (Table I). Lastly, myofibroblasts and adult ventricular fibroblasts did not express the endothelial cell markers VE-cadherin (Fig. 1) or eNOS (data not shown).

MYOFIBROBLASTS CAN SELF ASSEMBLE AND FORM LUMEN-LIKE STRUCTURES WHEN PLATED ON MATRIGEL

First passage scar myofibroblasts (n = 5) plated alone on matrigel in the absence of an exogenous angiogenic factor began to self assemble and form lumen-like structures (Fig. 2). The formation of lumen-like structures was also observed with 2nd and 3rd passage myofibroblasts (Fig. 2A–C). A temporal analysis revealed that the self assembly of lumen-like structures by myofibroblasts was detected at 2–4 h; a maximal response observed at ~8 h and persisted for at least 24 h (Fig. 2F). By contrast, neonatal (n = 3) and adult rat ventricular fibroblasts (n = 3) were unable to self assemble and form lumen-like structures when plated alone on matrigel (Fig. 2D,E).

SCAR MYOFIBROBLASTS DO NOT RECAPITULATE AN ENDOTHELIAL-LIKE PHENOTYPE IN THE PERI-INFARCT/INFARCT REGION

Despite the novel in vitro observation, additional experiments were required to assess whether the endothelial cell-like response of scar myofibroblasts plated on matrigel could be recapitulated in an in vivo setting. First passage myofibroblasts, isolated from the infarct region of 1-week post-MI rats were labeled with the fluorescent cell tracker CM-DiI, injected in the non-infarcted left ventricle of 3-day post-MI rats (n = 4) and engrafted rats sacrificed 7 days later. Injected myofibroblasts migrated to the scar and pockets of engrafted CM-DiI-labeled cells were detected throughout the peri-infarct/infarct region and often observed in close proximity to blood vessels, identified by eNOS (Fig. 3) and smooth muscle α-actin (Fig. 3) staining of endothelial cells and vascular smooth muscle cells, respectively. Within these pockets of engrafted cells, eNOS staining was not detected in CM-DiI-labeled myofibroblasts and CM-DiI-labeled vascular structures were not observed (Fig. 3). Engrafted CM-DiI-labeled myofibroblasts retained smooth muscle α-actin immunoreactivity (Fig. 3).

TGF-β AND ISOPROTERENOL PROMOTE MYOFIBROBLAST GROWTH AND CONCOMITANTLY SUPPRESS THE SELF ASSEMBLY OF LUMEN-LIKE STRUCTURES

The 24 h exposure of 1st passage scar myofibroblasts to TGF-β_3 (n = 4) led to a dose-dependent increase of protein synthesis characterized by the significant uptake of ^{3}H-leucine (Fig. 4A). By contrast, TGF-β_3 (n = 4) dose-dependently attenuated DNA synthesis in scar myofibroblasts as reflected by the significant inhibition of ^{3}H-thymidine uptake (Fig. 4B). The exogenous administration of TGF-β_1 (1 ng/ml) and TGF-β_3 (1 ng/ml) suppressed the self assembly and formation of lumen-like structures by scar myofibroblasts (n = 5) plated on matrigel (Fig. 4C). By contrast, the treatment of scar myofibroblasts with the TGF-β R1 kinase inhibitor II (100 nM) alone

TABLE I. Gene Expression in the Various Fibroblast Populations

	Neonatal ventricular fibroblasts (n = 5–6)	Adult ventricular fibroblasts (n = 3)	Scar myofibroblasts (n = 3–4)
Collagen α_1 Type 1	1.04 ± 0.06^a	0.45 ± 0.02	0.70 ± 0.07^a
TGF-β_1	0.98 ± 0.07	0.82 ± 0.07	1.14 ± 0.36
TGF-β_3	1.74 ± 0.5	1.12 ± 0.05	3.5 ± 0.29^b
CTGF	2.46 ± 0.46	2.37 ± 0.05	2.9 ± 0.44
VEGF	1.12 ± 0.12	0.96 ± 0.07	2.1 ± 0.29^b

Data expressed as mean ± SEM. Data were evaluated by a one-way ANOVA and a significant difference was determined by a Students–Neuman–Keuls multiple comparisons post hoc test.
[a] $P < 0.05$ versus adult.
[b] $P < 0.05$ versus adult and neonatal ventricular fibroblasts, and (n) number of independent cell preparations examined.

potentiated lumen-like structure formation (86 ± 20%↑ versus untreated; n = 3; $P < 0.05$ versus untreated).

The 24 h exposure of 1st passage myofibroblasts to the β-adrenergic receptor agonist isoproterenol (1 μM) significantly increased ^{3}H-thymidine (n = 5; Fig. 4D) and ^{3}H-leucine (n = 5) uptake (Fig. 4E). The pre-incubation with the PI3-K inhibitor LY294002 (10 μM; n = 5) or the mTOR inhibitor rapamycin (10 nM; n = 3) prior to isoproterenol administration inhibited DNA and protein synthesis (Fig. 4D,E). The pharmacological doses of LY294002 and rapamycin employed in the present study were previously shown to selectively abolish PI3-K signaling in neonatal rat ventricular fibroblasts [Colombo et al., 2003]. Moreover, the growth response induced by isoproterenol concomitantly inhibited the self assembly and formation of lumen-like structures by myofibroblasts plated on matrigel (Fig. 4C).

The inhibitory action of isoproterenol on the self assembly of lumen-like structures by myofibroblasts plated on matrigel may have occurred at least in part via the inhibition of F-actin filament reorganization. Within 1–2 h of treatment, isoproterenol initiated the rapid disassembly and/or depolymeristion of F-actin filaments in myofibroblasts (n = 3; Fig. 5B) as compared to untreated cells (Fig. 5A) that persisted for at least 8 h. Twenty-fours after

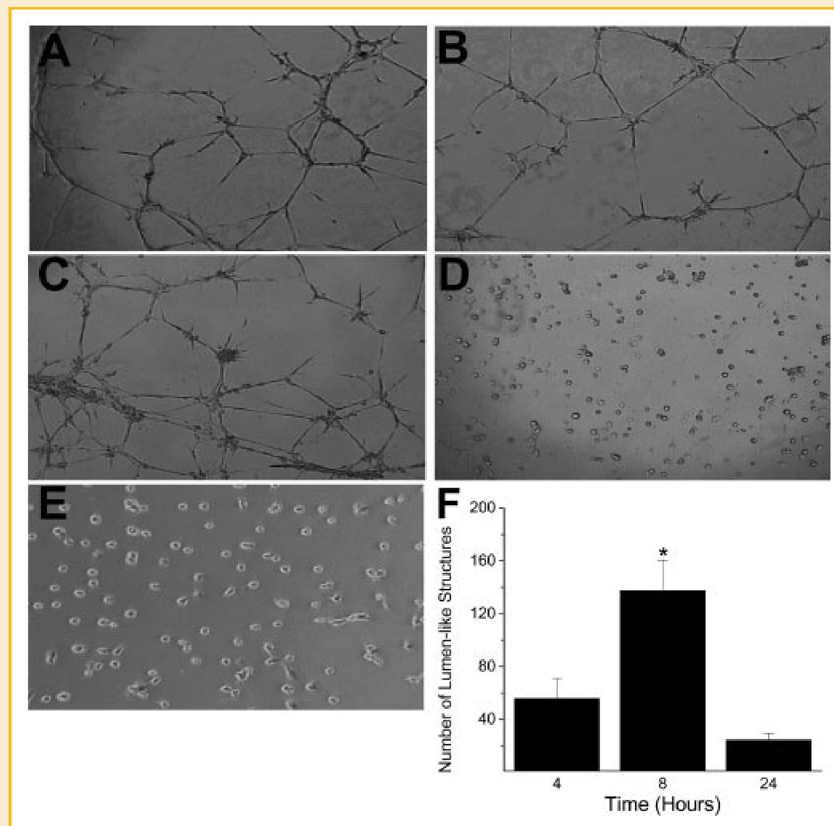

Fig. 2. Scar myofibroblasts self assemble and form lumen-like structures on matrigel. Panel A: The plating of 1st, (Panel B) 2nd, or (Panel C) 3rd passage scar myofibroblasts on matrigel in the absence of an exogenous angiogenic peptide initiated the self assembly and formation of lumen-like structures. By contrast, (Panel D) 1st passage neonatal and (Panel E) adult rat ventricular fibroblasts were unable to self assemble and form lumen-like structures when plated on matrigel. Panel F: Following the plating of scar myofibroblasts on matrigel (n = 5), lumen-like structures were detected within 2–4 h; a maximal response observed at 8 h and persisted for at least 24 h. $^*P<0.05$ versus 4 and 24 h.

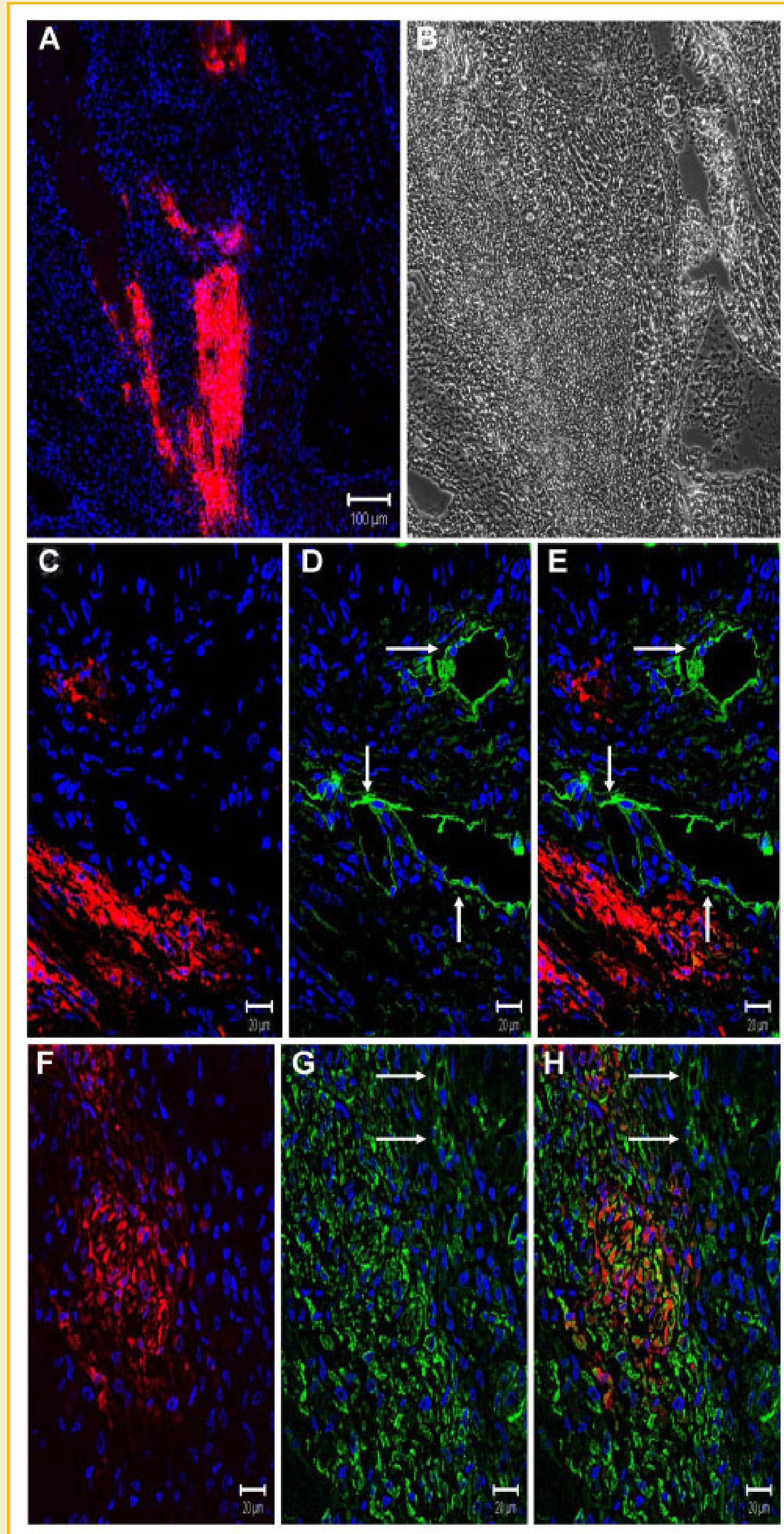

Fig. 3. The in vivo response of scar myofibroblasts injected into the infarcted rat heart. Panel A: CM-DiI-labeled myofibroblasts (red fluorescence) injected in the non-infarcted left ventricle of 3-day post-MI rats migrated to the infarct region. Panel B: Phase contrast picture of panel A. Panels C–E: CM-DiI-labeled myofibroblasts engrafted in the infarct region were detected in close proximity to eNOS$^{(+)}$ (indicated by arrow; green fluorescence) and (Panels F–H) smooth muscle α-actin$^{(+)}$ vessels (indicated by arrow; green fluorescence). However, engrafted myofibroblasts did not adopt an endothelial cell-like phenotype and failed to promote the de novo formation of CM-DiI-labeled blood vessels. Engrafted CM-DiI-labeled myofibroblasts retained smooth muscle-actin immunoreactive. The nucleus was identified with Top-PRO3 staining (blue fluorescence).

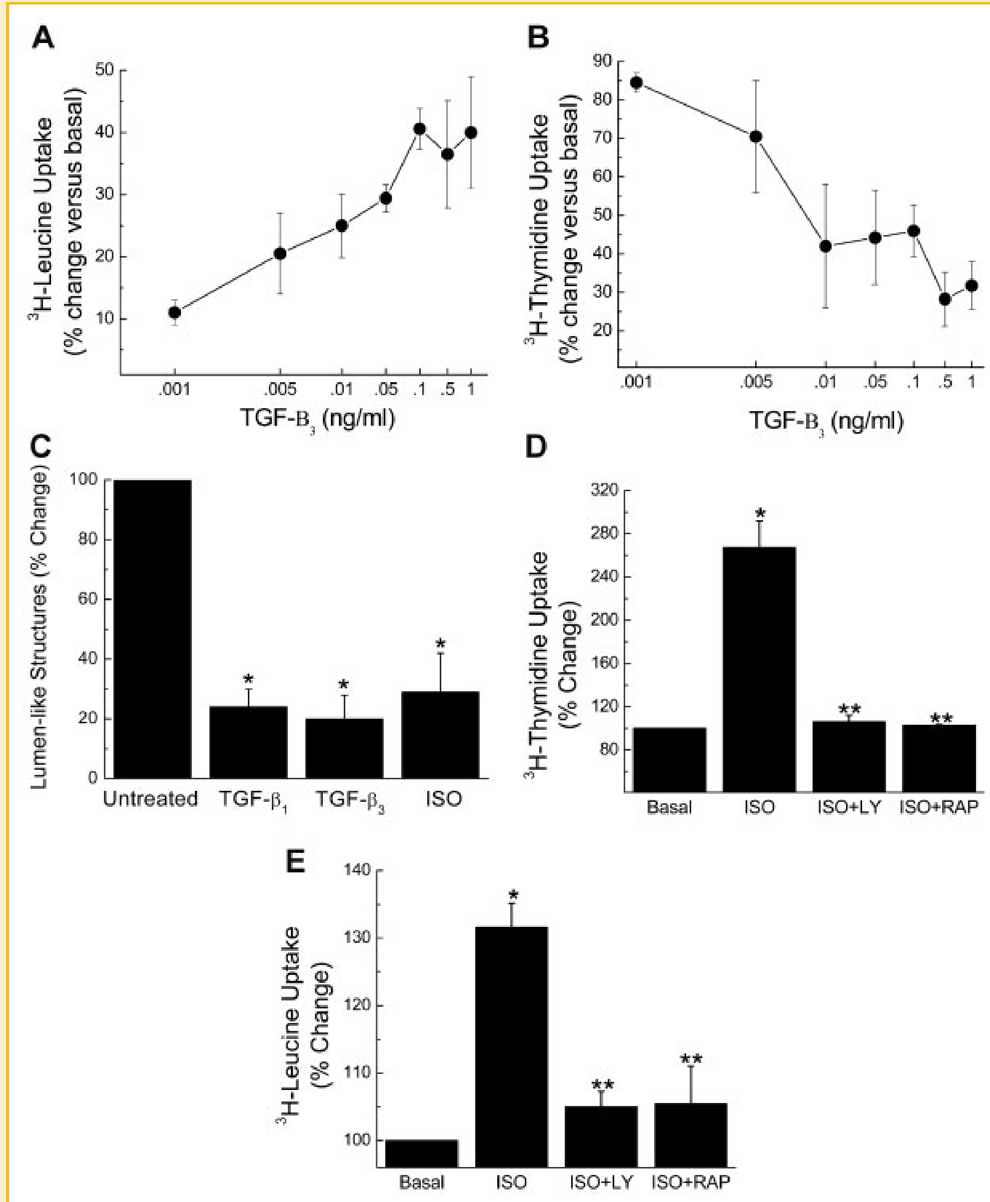

Fig. 4. TGF-β and isoproterenol on scar myofibroblast growth and lumen-like structure formation on matrigel. TGF-β_3 dose-dependently increased (Panel A) protein synthesis ($n = 4$) and concomitantly inhibited (Panel B) DNA synthesis ($n = 4$) of scar myofibroblasts. $^*P<0.05$ versus untreated. Isoproterenol (ISO; 1 μM; $n = 5$) stimulation increased (Panel C) ^{3}H-thymidine and (Panel D) ^{3}H-leucine uptake by scar myofibroblasts and inhibited by LY294002 (LY; 10 μM; $n = 5$) and rapamycin (RAP; 10 nM; $n = 3$). $^*P<0.05$ versus basal and $^{**}P<0.05$ versus isoproterenol. Panel E: TGF-β_1 (1 ng/ml), TGF-β_3 (1 ng/ml), and isoproterenol (1 μM) inhibited lumen-like structure formation by scar myofibroblasts plated on matrigel. The number of lumen-like structures formed at 8 h was set at 100%, and $^*P<0.05$ versus untreated.

isoproterenol administration, organized F-actin filaments were detected in myofibroblasts (data not shown). By contrast, TGF-β_1 (1 ng/ml) treatment for 1–2 h did not lead to the rapid disassembly and/or depolymeristion of F-actin filaments (Fig. 5C).

DISCUSSION

It has been well-established that the in vitro expansion of cardiac fibroblasts leads to the induction of smooth muscle α-actin [Colombo et al., 2003; Beguin et al., 2012]. Consistent with these data, cultured scar myofibroblasts, neonatal, and adult ventricular rat fibroblasts express smooth muscle α-actin and the level of expression comparable among the three populations. In addition, scar myofibroblasts, neonatal and adult ventricular fibroblasts express collagen α_1 type 1 and a panel of peptide growth factor mRNAs. However, collagen α_1 type 1, VEGF-A, and TGF-β_3 mRNA levels were significantly greater in scar myofibroblasts versus normal adult ventricular fibroblasts and these findings consistent with their seminal role during reparative fibrosis [Micera et al.,

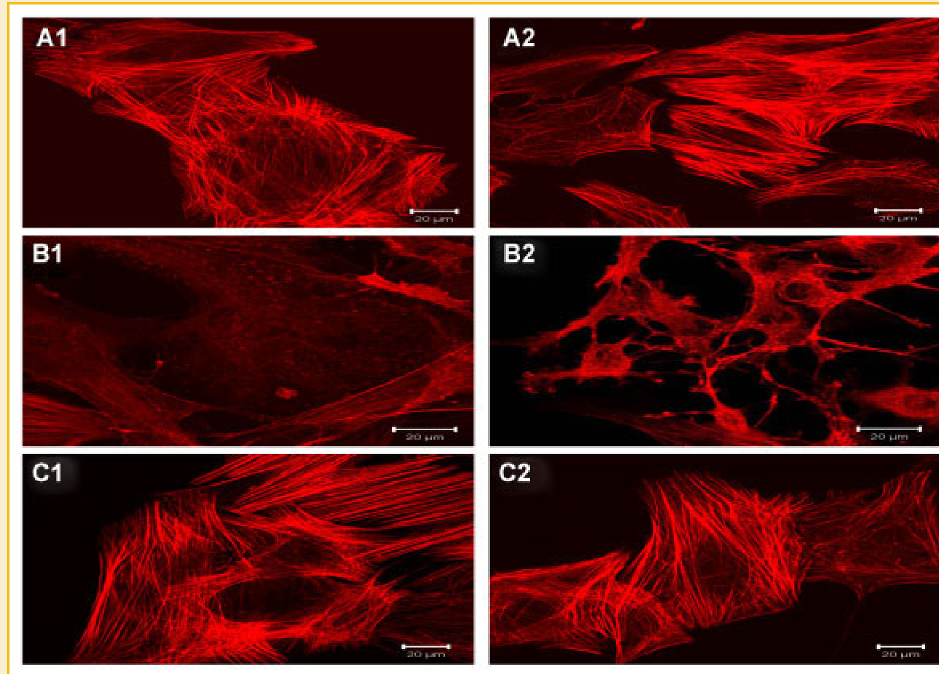

Fig. 5. F-actin filament disassembly and/or depolymerization in scar myofibroblasts. Panels A: Phalloidin staining revealed organized F-actin filaments in untreated myofibroblasts. Panels B: Isoproterenol (1 μM) treatment of myofibroblasts led to the disassembly and/or depolymerization of F-actin filaments 1–2 h after administration that persisted for at least 8 h. Panels C: TGF-β_1 (1 ng/ml) treatment of myofibroblasts for 1–2 h did not lead to the disassembly and/or depolymerization of F-actin filaments.

2001; Zhao and Eghbali-Webb, 2001; Chintalgattu et al., 2003; Dai et al., 2005; Hasan et al., 2006; Cimini et al., 2007; van Amerongen et al., 2008; El-Helou et al., 2008b; Pilla et al., 2009; Liam et al., 2009]. The cardiac fibroblast populations can also be distinguished by nestin expression, as the intermediate filament protein was highly expressed in neonatal rat ventricular fibroblasts, significantly downregulated in adult ventricular fibroblasts and re-induced in a subpopulation of scar myofibroblasts [Beguin et al., 2012]. The present study has further demonstrated that scar myofibroblasts plated alone on matrigel in the absence of an angiogenic peptide were capable of self assembly and formation of lumen-like structures akin to that reported by endothelial cells [Geraldes et al., 2007]. By contrast, neither neonatal nor adult ventricular fibroblasts were capable of recapitulating an endothelial cell-like response when plated on matrigel. Thus, their ability to self assemble and form lumen-like structures on matrigel provides additional novel data further distinguishing scar myofibroblasts from normal rat ventricular fibroblasts.

Despite the in vitro observation, additional experiments were required to assess whether the recapitulation of an endothelial cell-like response by scar myofibroblasts was translated to the in vivo setting. First passage scar myofibroblasts were labeled with the non-diffusible fluorescent tracker CM-DiI and injected in the viable myocardium of a 3-day post-MI rat. An identical approach was employed to track the fate of cardiac neural stem cells injected into the viable myocardium of the infarcted rat heart. Injected fluorescent-labeled cardiac nestin$^{(+)}$ neural stem cells migrated to the scar, differentiated to a vascular cell and led to the formation of de novo blood vessels [El-Helou et al., 2008a]. In the present study, CM-DiI-labeled scar myofibroblasts were injected in the viable myocardium of a 3-day post-MI rat and 7 days later migrated to the peri-infarct/infarct region. Engrafted CM-DiI-labeled scar myofibroblasts were predominantly detected in close proximity to eNOS/smooth muscle α-actin immunoreactive blood vessels. However, engrafted CM-DiI-labeled myofibroblasts were unable to adopt an endothelial cell-like phenotype and the de novo formation of CM-DiI-labeled small calibre blood vessels was likewise not observed in the peri-infarct/infarct region. Engrafted CM-DiI-labeled myofibroblasts retained smooth muscle α-actin immunoreactivity. The latter findings were not entirely unexpected as reduced myofibroblast proliferation and/or decreased synthesis and deposition of extracellular matrix proteins leads to inadequate scar healing, left ventricular dilation and adverse cardiac remodelling [Dai et al., 2005; Cimini et al., 2007; van Amerongen et al., 2008; El-Helou et al., 2008b; Liam et al., 2009; Pilla et al., 2009]. Thus, preferential use of the myofibroblast population as a substrate of angiogenesis during the early phase of the reparative fibrotic response would be maladaptive.

The failure of engrafted myofibroblasts to adopt an endothelial cell-like phenotype suggests that the restrictive nature of the peri-infarct/infarct region may be secondary to the expression of local stimuli. Transforming growth factor-β is highly expressed in the scar, plays a seminal role in the differentiation of fibroblasts to smooth muscle α-acin$^{(+)}$ myofibroblasts and promotes a secretory phenotype [Willems et al., 1994; Sun et al., 2000; Frangogiannis et al., 2002; Virag and Murry, 2003; Squires et al., 2005; Wynn,

2008; Porter and Turner, 2009]. The peri-infarct/infarct region is also innervated by sympathetic fibres and β-adrenergic agonists were reported to stimulate neonatal and adult rat ventricular fibroblast growth in part via a PI3-K-dependent pathway [Kim et al., 2002; Colombo et al., 2003; Hasan et al., 2006; El-Helou et al., 2008b]. The exposure of scar myofibroblasts to TGF-β_3 favoured a secretory phenotype characterized by increased protein synthesis and the concomitant attenuation of DNA synthesis [Porter and Turner, 2009]. Isoproterenol treatment of myofibroblasts increased both ^{3}H-leucine and ^{3}H-thymidine uptake and attenuated by the PI3-K inhibitor LY294002 and the mTOR inhibitor rapamycin. The secretory phenotype favoured by TGF-β_3 was associated with the concomitant inhibition of lumen-like structure formation by myofibroblasts plated on matrigel and an analogous suppressive effect was observed with TGF-β_1. By contrast, the TGF-β R1 kinase inhibitor II potentiated the formation of lumen-like structures by scar myofibroblasts. It remains unknown if the inhibitory action of TGF-β R1 kinase inhibitor II was secondary to TGF-β released by scar myofibroblasts and/or present on matrigel complex. Likewise, the growth response initiated by isoproterenol concomitantly inhibited the self assembly and formation of lumen-like structures by myofibroblasts. The latter suppressive action by isoproterenol may be related at least in part to the rapid disassembly and/or depolymerization of F-actin filaments as their reorganization was reported to represent a requisite event for endothelial cell migration and angiogenesis (van Nieuw Amerongen et al., 2003; Dufourcq et al., 2008). Collectively, these data demonstrate that the self assembly and formation of lumen-like structures by myofibroblasts plated on matrigel was sensitive TGF-β and isoproterenol inhibition.

The prevailing dogma states that normal cardiac fibroblasts migrate to the infarct region and under the influence of TGF-β, differentiate to myofibroblast phenotype characterized by smooth muscle α-actin expression [Willems et al., 1994; Sun et al., 2000; Frangogiannis et al., 2002; Virag and Murry, 2003; Squires et al., 2005; Wynn, 2008]. However, at least one study has demonstrated that a subpopulation of myofibroblasts residing in the infarct region of the ischemically damaged heart was derived from cells originating from the bone marrow [van Amerongen et al., 2008]. The accumulation of fibroblasts in numerous damaged tissues was also reported to be secondary to epithelial cell differentiation through a process referred to as epithelial–mesenchymal transition [Zeisberg et al., 2003; Jain et al., 2007]. A related phenomenon was identified in the fibrotic mouse heart, as TGF-β_1 induced endothelial cell differentiation to smooth muscle α-actin$^{(+)}$ myofibroblasts [Zeisberg et al., 2007]. In addition, a recent study has demonstrated that a subpopulation of smooth muscle α-actin$^{(+)}$ myofibroblasts detected in the scar of the infarcted mouse heart originated from endothelial cells [Aisagbonhi et al., 2011]. Moreover, epithelial- and endothelial–mesenchymal transition can be antagonized or reversed [Zeisberg et al., 2003, 2007]. The present study has demonstrated that rat scar myofibroblasts can recapitulate an endothelial cell-like response when plated on matrigel and sensitive to TGF-β inhibition. These data indirectly support the premise that the accumulation of scar myofibroblasts in the infarcted rat heart during the early phase of reparative fibrosis may have originated at least in part from endothelial–mesenchymal transition.

ACKNOWLEDGMENTS

I would like to thank France Thériault for excellent secretarial assistance.

REFERENCES

Aisagbonhi O, Rai M, Ryzhov S, Atria N, Feoktistov I, Hatzopoulos AK. 2011. Experimental myocardial infarction triggers canonical Wnt signaling and endothelial-to-mesenchymal transition. Dis Model Mech 4:469–483.

Beguin P, Gosselin H, Mamarbachi M, Calderone A. 2012. Nestin expression is lost in ventricular fibroblasts during postnatal development of the rat heart and re-expressed in scar myofibroblasts. J Cell Physiol 227:813–820.

Calderone A, Bel-Hadj S, Drapeau J, El-Helou V, Gosselin H, Clement R, Villeneuve L. 2006. Scar myofibroblasts of the infarcted rat heart express natriuretic peptides. J Cell Physiol 207:165–173.

Campbell TN, Attwell S, Arcellana-Panlilio M, Robbins SM. 2006. Ephrin A5 expression promotes invasion and transformation of murine fibroblasts. Biochem Biophys Res Commun 350:623–628.

Chintalgattu V, Nair DM, Katwa LC. 2003. Cardiac myofibroblasts: A novel source of vascular endothelial growth factor (VEGF) and its receptors Flt-1 and KDR. J Mol Cell Cardiol 35:277–286.

Cimini M, Fazel S, Zhuo S, Xaymardan M, Fujii H, Weisel RD, Li RK. 2007. c-Kit dysfunction impairs myocardial healing after infarction. Circulation 116(11 suppl):I77–I82.

Colombo F, Gosselin H, El-Helou V, Calderone A. 2003. (-adrenergic receptor-mediated DNA synthesis in cardiac fibroblasts proceeds via a phosphatidylinositol 3-kinase dependent pathway refractory to the antiproliferative action of cyclic AMP. J Cell Physiol 195:322–330.

Dai W, Wold LE, Dow JS, Kloner RA. 2005. Thickening of the infarcted wall by collagen injection improves left ventricular function in rats. J Am Coll Cardiol 46:714–719.

Dufourcq P, Leroux L, Ezan J, Descamps B, Lamazière JM, Costet P, Basoni C, Moreau C, Deutsch U, Couffinhal T, Duplàa C. 2008. Regulation of endothelial cell cytoskeletal reorganization by a secreted frizzled-related protein-1 and frizzled 4- and frizzled 7-dependent pathway: Role in neovessel growth. Am J Pathol 172:37–49.

El-Helou V, Beguin PC, Assimakopoulos J, Clement R, Gosselin H, Brugada R, Aumont A, Biernaskie J, Villeneuve L, Leung TK, Fernandes KJ, Calderone A. 2008a. The rat heart contains a neural stem cell population; role in sympathetic sprouting and angiogenesis. J Mol Cell Cardiol 45:694–702.

El-Helou V, Proulx C, Gosselin H, Clement R, Mimee A, Villeneuve L, Calderone A. 2008b. Dexamethasone treatment of post-MI rats attenuates sympathetic innervation of the infarct region. J Appl Physiol 104:150–156.

Frangogiannis NG, Smith CW, Entman ML. 2002. The inflammatory response in myocardial infarction. Cardiovasc Res 53:31–47.

Geraldes P, Gosselin H, Tanguay JF, Clément R, Calderone A. 2007. Tamoxifen treatment of myocardial infarcted female rats exacerbates scar formation. Pflugers Arch 454:385–393.

Hasan W, Jama A, Donohue T, Wernli G, Onyszchuk G, Al-Hafez B, Bilgen M, Smith PG. 2006. Sympathetic hyperinnervation and inflammatory cell NGF synthesis following myocardial infarction in rats. Brain Res 1124:142–154.

Jain R, Shaul PW, Borok Z, Willis BC. 2007. Endothelin-1 induces alveolar epithelial-mesenchymal transition through endothelin type A receptor–mediated production of TGF-β1. Am J Respir Cell Mol Biol 37:38–47.

Kim J, Eckhart AD, Eguchi S, Koch WJ. 2002. Beta-adrenergic receptor-mediated DNA synthesis in cardiac fibroblasts is dependent on transactivation of the epidermal growth factor receptor and subsequent activation of extracellular signal-regulated kinases. J Biol Chem 277:32116–32123.

Liam PR, Matsuzaki K, Noma M, Jackson BM, Eperjesi TJ, Plappert TJ, St John-Sutton MG, Gorman JH 3rd, Gorman RC. 2009. Dermal filler injection:

A novel approach for limiting infarct expansion. Ann Thorac Surg 87:148–155.

Micera A, Vigneti E, Pickholtz D, Reich R, Pappo O, Bonini S, Maquart FX, Aloe L, Levi-Schaffer F. 2001. Nerve growth factor displays stimulatory effects on human skin and lung fibroblasts, demonstrating a direct role for this factor in tissue repair. Proc Natl Acad Sci 98:6162–6167.

Pilla JJ, Gorman JH III, Gorman RC. 2009. Theoretic impact of infarct compliance on left ventricular function. Ann Thorac Surg 87:803–810.

Porter KE, Turner NA. 2009. Cardiac fibroblasts; at the heart of myocardial remodelling. Pharmacol Ther 123:255–278.

Sotgia F, Del Galdo F, Casimiro MC, Bonuccelli G, Mercier I, Whitaker-Menezes D, Daumer KM, Zhou J, Wang C, Katiyar S, Xu H, Bosco E, Quong AA, Aronow B, Witkiewicz AK, Minetti C, Frank PG, Jimenez SA, Knudsen ES, Pestell RG, Lisanti MP. 2009. Caveolin-1$^{-/-}$ null mammary stromal fibroblasts share characteristics with human breast cancer-associated fibroblasts. Am J Pathol 174:746–761.

Squires CE, Escobar GP, Payne JF, Leonardi RA, Goshorn DK, Sheats NJ, Mains IM, Mingoia JT, Flack EC, Lindsey ML. 2005. Altered fibroblast function following myocardial infarction. J Mol Cell Cardiol 39:699–707.

Strakova Z, Livak M, Krezalek M, Ihnatovych I. 2008. Multipotent properties of myofibroblast cells derived from human placenta. Cell Tissue Res 332:479–488.

Sun Y, Zhang JQ, Zhang J, Lamparter S. 2000. Cardiac remodelling by fibrous tissue after infarction in the rat. J Lab Clin Med 135:316–323.

van Amerongen MJ, Bou-Gharios G, Popa ER, van Ark J, Petersen AH, van Dam GM, van Luyn MJA, Harmsen MC. 2008. Bone marrow-derived myofibroblasts contribute functionally to scar formation after myocardial infarction. J Pathol 214:377–386.

van Nieuw Amerongen GP, Kollwijk P, Versteilen A, van Hinsbergh VW. 2003. Involvement of RhoA/Rho kinase signaling in VEGF-induced endothelial cell migration and angiogenesis in vitro. Arterioscler Thromb Vasc Biol 23:211–217.

Virag T, Murry CH. 2003. Myofibroblast and endothelial cell proliferation during murine myocardial infarct repair. Am J Pathol 163:2433–2440.

Willems IE, Havenith MG, De Mey JG, Daemen MJ. 1994. The alpha-smooth muscle actin-positive cells in healing human myocardial scars. Am J Pathol 145:868–875.

Wynn T. 2008. Cellular and molecular mechanisms of fibrosis. J Pathol 214:199–210.

Zeisberg EM, Tarnavski O, Zeisberg M, Dorfman AL, McMullen JR, Gustafsson E, Chandraker A, Yuan X, Pu WT, Roberts AB, Neilson EG, Sayegh MH, Izumo S, Kalluri R. 2007. Endothelial-to-mesenchymal transition contributes to cardiac fibrosis. Nat Med 13:952–961.

Zeisberg M, Hanai J, Sugimoto H, Mammoto T, Charytan D, Strutz F, Kalluri R. 2003. BMP-7 counteracts TGF-beta1-induced epithelial-to-mesenchymal transition and reverses chronic renal injury. Nat Med 9:964–968.

Zhao L, Eghbali-Webb M. 2001. Release of pro- and anti-angiogenic factors by human cardiac fibroblasts: Effects on DNA synthesis and protection under hypoxia in human endothelial cells. Biochim Biophys Acta 1538:273–282.